Fuel 212 (2018) 576–585

Contents lists available at ScienceDirect

Fuel

journal homepage: www.elsevier.com/locate/fuel

Experimental and theoretical study of oxidative stability of alkylated furans used as gasoline blend components

Earl Christensen[a,*], Gina M. Fioroni[a], Seonah Kim[a,*], Lisa Fouts[a], Erica Gjersing[a], Robert S. Paton[b], Robert L. McCormick[a]

[a] National Renewable Energy Laboratory, 15013 Denver West Parkway, Golden, CO 80401-3305, USA
[b] Chemistry Research Laboratory, University of Oxford, 12 Mansfield Road, Oxford OX1 3TA, UK

GRAPHICAL ABSTRACT

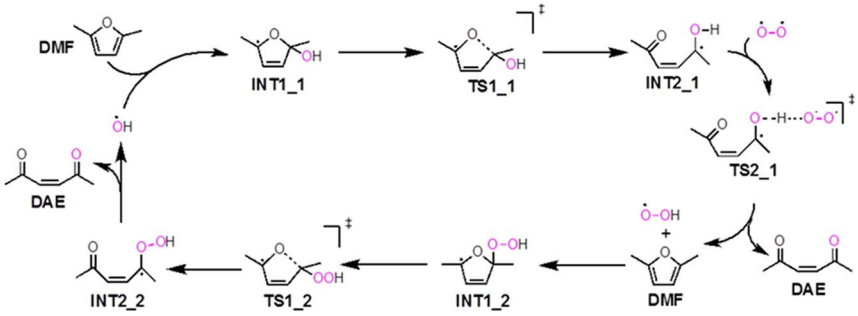

ARTICLE INFO

Keywords:
Alkyl furan
Methylfuran
Dimethylfuran
Gasoline
Oxidation stability

ABSTRACT

Alkylated furans such as 2,5-dimethylfuran and 2-methylfuran can be produced from biomass and have very attractive properties for use as spark-ignition fuel blendstocks. Their high octane numbers, relatively high energy density, low water solubility, and minimal effect on gasoline blend volatility are potentially significant advantages over alcohol-based fuels. However, prior studies have reported poor oxidative stability for furanic compound-gasoline blends, as well as the potential for the formation of dangerous organic peroxides. We show that alkylated furans have very low oxidative stability compared to conventional gasoline. Upon oxidation they form highly polar ring-opening products that can react with the starting furanic compound to form dimers, trimers, and higher polymers with intact furan rings. Dimers of the starting furan compounds were also observed. These gasoline-insoluble gums can be problematic for fuel storage or in vehicle fuel systems. Evaporation to dryness under ambient conditions also produced gum with similar composition. Gums produced via evaporation were found to contain peroxides; however, whether these pose a threat of shock initiated explosion has not been determined. We also propose a density functional theory-based analysis of possible reaction pathways, showing that OH radicals can form by reaction of the alkyl group and that addition of OH radicals to the furan ring is energetically favored and leads to ring opening products. Antioxidant additives can be effective at limiting the oxidation reaction in gasoline, but require much higher concentrations than are commonly used in commercial gasolines.

* Corresponding authors.
E-mail addresses: earl.christensen@nrel.gov (E. Christensen), seonah.kim@nrel.gov (S. Kim).

http://dx.doi.org/10.1016/j.fuel.2017.10.066
Received 10 September 2017; Received in revised form 10 October 2017; Accepted 12 October 2017
Available online 06 November 2017

1. Introduction

Furanic compounds, specifically 2,5-dimethyfuran (DMF) and 2-methylfuran (MF), have long been of interest as potential biofuels. Their boiling point, high octane number, relatively high heating value, low solubility in water, and minimal effect on gasoline blend volatility make them very attractive as components of fuels for spark-ignition engines (Table 1) [1,2]. It is particularly notable that these compounds exhibit very high blending octane numbers when blended into petroleum blendstocks, making them among the most attractive proposed biofuels for enabling the design and production of spark-ignition engines with significantly improved efficiency [2]. These compounds can be produced from lignocellulosic biomass via several different routes [3–8]. In one approach, DMF is produced from the C6 sugar fructose by dehydration to form hydroxymethylfurfural, which is then hydrogenated. Production from cellulose (a polymer of glucose), therefore, requires initial isomerization of glucose to fructose. MF can be produced from the C5 sugar xylose by dehydration to furfural followed by hydrogenation. A practical process for conversion of lignocellulosic biomass containing both cellulose and hemicellulose (a polymer of xylose) would produce a mixture of DMF and MF [9,10]. The combustion of DMF and MF has also been extensively studied theoretically [11,12], in fundamental experiments [13–15], and in engine combustion experiments [16–21].

Only a few studies have examined how these promising high-octane number compounds affect practical fuel properties when blended with conventional petroleum-derived gasoline blendstocks. Christensen and coworkers blended DMF and MF into a petroleum-derived hydrocarbon gasoline blendstock intended for blending with 10 vol% ethanol [1]. Blending of MF (11 percent by volume (vol%)) and DMF (13 vol%) showed little effect on vapor pressure and a 5–10 °C depression in the 50% evaporation temperature (T50) with no significant effect on T10 or T90, all very desirable properties for gasoline blending. Blends were very stable in the presence of water with no phase separation or uptake of oxygenate by the water phase. Very high volumetric blending research octane numbers of about 150 were observed at this blend level in the 85 research octane number blendstock.

Researchers at Shell Global Solutions conducted a detailed evaluation of MF as a gasoline component, reporting similar fuel property effects to those described above [23]. They also noted that MF blending degraded the oxidation stability of the fuel as measured by ISO 6246 (a standard test for measuring the oxidation stability and gum formation for gasoline), and furthermore noted increased inlet valve and injector deposits in a three-car, 90,000-km on-road test. In a previous study we reported that DMF blending can negatively impact gasoline stability, producing high levels of insoluble gum on the ASTM International (ASTM) D873 gum formation test for blends as low as 10 vol%, and failing the ASTM D525 oxidation stability test for a 20 vol% blend [24]. These standard stability tests are conducted at 100 °C under 700 kPa initial pressure of oxygen.

Additionally, Fabos and coworkers examined the formation of peroxides during storage of bio-derived oxygenates including DMF and found that this compound increases in peroxide number over time similar to tetrahydrofuran (THF), which is a known peroxide former [25]. Interestingly, furan did not form high levels of peroxides. The formation of peroxides via oxidation at ambient conditions is a considerable safety concern as some organic peroxides can present an explosion hazard when exposed to physical shock. Many common laboratory solvents are known to form peroxides, and precautions are recommended that allow for their safe storage and handling. These precautions include protection from light and air, the use of free radical scavenging additives, as well as periodic monitoring for peroxide formation [26]. Petroleum-derived gasolines containing olefins are also known to form peroxides during storage, which degrades octane ratings and, if sufficient oxidation occurs, gums can form causing filter plugging and engine deposits [27]. Prevention of oxidation during fuel storage is vital for maintaining fuel quality.

Here we describe the results of an experimental and theoretical study examining the oxidation stability of furanic compounds within the contexts of both gasoline stability and peroxide formation as a safety issue.

Table 1
Important fuel properties of DMF and MF.

Property	DMF	MF
Boiling point, °C	94	65
Research octane number [22]	101	103
Motor octane number [22]	88	86
Molar blending research octane number [1][1]	137	131
Molar blending motor octane number [1]	102	101
Lower heating value, MJ/L	30.1	27.6
Water solubility, mg/L	1460	3410

[1] Molar blending octane numbers are for 11.3 vol% MF or 13.4 vol% DMF in a sub-octane gasoline blendstock, as described in more detail in Ref. [1].

2. Methods

2.1. Experimental

Furan, MF, DMF, and 2-ethylfuran (EF) with purity ≥99% were purchased from Sigma Aldrich. Furan and MF were received containing 250 ppm (ppm) butylated hydroxytoluene stabilizer. DMF and EF were purchased without added stabilizers. Each compound was passed over a bed of silica to remove oxidation products, stabilizers, and other polar materials before use. DMF and MF as received exhibited a yellow color, which was removed by the silica resulting in a clear liquid. Blends for testing were prepared gravimetrically with 2,2,4-trimethylpentane (iso-octane, purchased from VWR) to 10 vol% concentration.

Oxidation stability of blends was assessed at 100 °C under an initial pressure (at room temperature) of 700 kPa of oxygen. These are the test conditions of the ASTM D525 test used to measure the oxidation induction time (or breakpoint) of commercial gasolines. The test is run for 24 h while the pressure of the vessel is monitored for a breakpoint defined by a rate of pressure decrease of greater than 14 kPa per 15 min, which defines the induction period of the sample. A minimum induction time of 240 min is required for commercial gasoline in the United States. The final pressure at 24 h is reported, and the liquid phase is recovered for analysis. A gasoline gum formation test, ASTM D873, is conducted in the same apparatus at the same conditions for a fixed period of time – 24 h was used in this study. This is followed by solvent rinsing (50:50 by volume mixture of toluene and acetone), evaporation, and weighing of gum formed during oxidation.

In some cases, the DMF blend was treated with a mixture of proprietary antioxidants at the concentrations recommended by the manufacturer for effective gasoline stabilization. The antioxidant mixture contained phenylenediamine-based and hindered-phenol based components that were added to a 10 vol% DMF blend at concentrations of 10 and 30 ppm, respectively. An additional 10 vol% DMF blend was tested with 10 times the recommended concentration of these antioxidants (100 and 300 ppm).

Gum and peroxide formation at room temperature during furanic compound evaporation was assessed by allowing 100 mL of neat MF and DMF to evaporate in 250-mL Erlenmeyer flasks in a fume hood. Peroxides were measured following a modified version of ASTM method D3703 for peroxide number of gasoline, jet fuel, and diesel. This method was modified for potentiometric endpoint detection rather than colorimetric titration. The method has been modified for the use of potentiometric end point detection in the place of colorimetric titration to provide improved precision and throughput via use of an instrument based endpoint opposed to human eye detection of color change. Accuracy of the method with this modification was verified by

Table 2
Results of oxidation at 100 °C under 700 kPa of O_2 initial pressure. Induction time (or breakpoint) measurement according to ASTM D525. Gum formation by ASTM D873 run for 24 h.

Blend, 10 vol% in iso-octane	Breakpoint, minutes	Pressure drop, kPa	Total potential gum, mg/100 mL
Furan	> 1440	46	33
MF	630	390	1065
MF, under N_2	> 1440	126	6
EF	94	257	1441
DMF	66	562	774
DMF, D873 Replicate	NA	NA	573
DMF with antioxidants	81	558	550
DMF with 10x antioxidants	397	614	733

examining samples containing known levels of t-butylperoxide.

Degradation products were characterized using several methods. In general, these are qualitative, or at best semi-quantitative, assessments of composition rather than standard measurements with known uncertainty. Gas chromatography with mass spectrometric detection (GC–MS) was conducted on the iso-octane blends and acetone solutions of the gums formed after 24 h at 100 °C and 700 kPa O_2 initial pressure. An Agilent 7890A GC coupled with an Agilent 5975C mass selective detector (MSD) equipped with an Agilent DB-5MS column (5% phenyl polydimethylsiloxane phase with dimensions: 30 m × 0.25 mm, 0.25 μm d_f) was used for GC–MS analyses. The injection port temperature was set at 275 °C with helium carrier gas flow rate of 1 mL/min and an injection split ratio of 100:1. Injection volume was 1 μL. Oven temperature was held at 45 °C for 5 min followed by a ramp of 10 °C/min to 100 °C followed by 25 °C/min a final temperature of 320 °C. The MSD was operated in continuous scan mode from *m/z* 35 to 500, and the transfer line temperature was held at 350 °C. Peaks detected were tentatively identified by comparison to the National Institute of Standards and Technology 2011 library of mass spectra with NIST MS Search 2.0 software.

Molecular weight ranges of gums were determined with gel permeation chromatography (GPC) using a Waters Acquity ultra-performance liquid chromatograph equipped with a refractive index detector (RID). The columns used for compound separation by molecular weight were Waters Acquity APC XT 200, 125, and 45 Å (4.6 × 75 mm, 2.5 μm), and the mobile phase was THF at a flow rate of 1 mL/min. Column and RID temperatures were maintained at 30 °C. A relative molecular weight calibration was generated with polyethylene glycol standards, Mp 102 – 40,000 Da purchased from Sigma Aldrich. The injection volume was 7 μL. The calibration curve was found to have $R^2 = 0.998$ across the molecular weight range. Samples were dissolved in THF at a concentration of approximately 5 mg/mL for injection onto the chromatograph.

Direct analysis in real time ionization with time-of-flight mass spectrometry (DART-TOF MS) was used to analyze gums collected from ASTM D873 oxidation. A JEOL AccuTOF time-of-flight MS equipped with an Ionsense DART ion source was used to collect spectra at a rate of 1 per second in the *m/z* range of 70–1200. The MS resolving power was 6000 (FWHM) for protonated reserpine at *m/z* 609.281. The TOF atmospheric pressure interface was operated in positive ion mode with the following parameters: orifice 1 = 20 V, ring lens = orifice 2 = 5 V. A sample of polyethylene glycol with average molecular weight 600 (PEG 600, purchased form Sigma Aldrich) dissolved in methanol was measured with each data file as a reference standard for internal mass calibration. The DART source was operated with helium, and the gas heater was set to 300 °C. Mass calibration, centroiding, spectral averaging, and background subtraction were carried out using Shrader Software Solutions TSSPro3 software. Mass spectra were analyzed using Mass Mountaineer software (RBC Software).

Nuclear magnetic resonance spectroscopy (NMR) was conducted on gum samples. Each gum was prepared by adding 0.4 mL of $CDCl_3$ to the vials containing dried products. The NMR spectra were acquired on a Bruker Avance III 600 MHz spectrometer (14.1 T magnet, ^{13}C = 150.9254 MHz, and ^{1}H = 600.1628 MHz) with a BBO 5-mm probe. ^{13}C NMR spectra were acquired with a 30° pulse (90° = 10 μs), waltz 16 proton decoupling, and a recycle delay of 2 s. The ^{1}H spectra were acquired with a 90° pulse (15.3 μs), recycle delay of 10 s, and 32 scans.

2.2. Theory

Quantum chemical calculations were performed with density functional theory. All reactants, intermediates, transition state structures and products were optimized at the B3LYP/6-31G(2df,p) level of theory. Each minimum has all real frequencies and each transition structure has only one imaginary frequency. Intrinsic reaction coordinate calculations were performed to confirm that transition structures connect the relevant energy minima. We used all B3LYP/-31G(2df,p) optimized geometries and frequencies to perform Gaussian-4 (G4) composite *ab initio* calculations [28] at 298.15 K. G4 formation enthalpies for a series of radicals containing C, H and O gave a mean unsigned error of 1.7 kJ/mol (0.41 kcal/mol) against the experimental values recommended in the Active Thermochemical Tables [28–30]. However, it is not straightforward to estimate the error for an arbitrary reaction. The benchmark errors are for heats of formation. The reactions and barriers calculated here will be (on average) larger errors – since they are effectively calculated from differential heats of formation. The G4 values are thermal-corrected energies (which is related to the enthalpy by H = U + PV). All calculations were performed with Gaussian 09 [31].

3. Results

3.1. Oxidation experiments

Results of induction time and gum formation measurement at

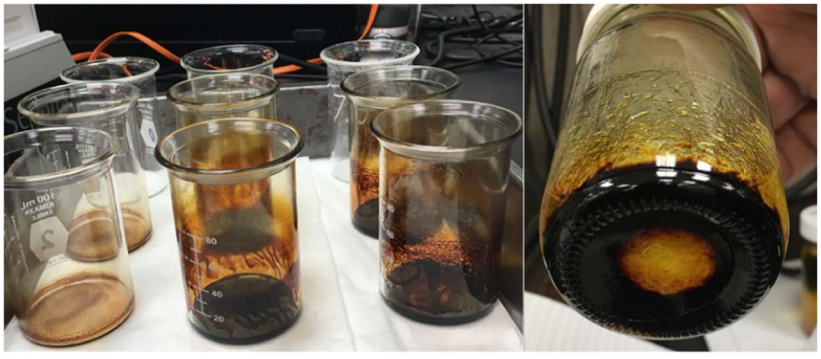

Fig. 1. Gum produced after 24 h at 100 °C under 700 kPa O_2 initial oxygen pressure (ASTM D873 method) for 10 vol% blends in iso-octane: furan (left), EF (center), MF (right), and DMF (far right).

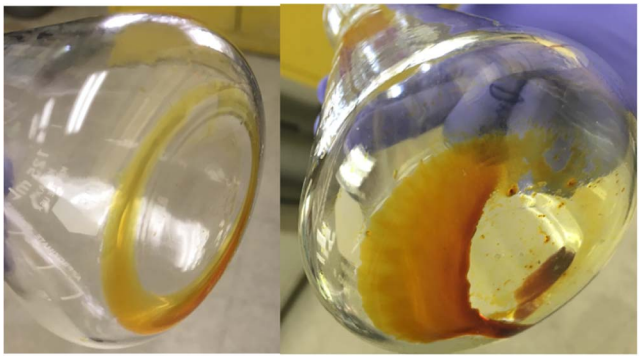

Fig. 2. Gum produced after evaporation of 100 mL of neat furanic compound at ambient conditions: MF (left) and DMF (right).

100 °C/700 kPa O_2 initial pressure are shown in Table 2, and a photograph of the resulting gums is Fig. 1. Little to no reaction is observed with furan, but all of the alkyl furans oxidized and formed significant amounts of gum. A test under nitrogen conducted for MF showed no reaction. Note that the levels of gums observed for the alkyl furan blends are 10–100 times higher than would be observed for a conventional gasoline [24].

The MF blend has a long induction time (or breakpoint), easily meeting the ASTM requirement of 240 min, but produces over 1000 mg/100 mL of gum. The run under nitrogen clearly shows that oxygen is required for gum formation. This is consistent with the observation (shown below) that gums from MF consist of ring opening and condensation products that incorporate some oxygen. For EF we also see a very high gum level of 1441 mg/100 mL, but the induction time is very short at 94 min, suggesting rapid incorporation of large amounts of oxygen in the products. For DMF we see a short induction time but a significantly lower level of gum. A replicate DMF gum result differs from the first run by 200 mg/mL giving some indication of the reproducibility of this experiment at these very high gum levels. At gum levels more typical of conventional gasolines (5–20 mg/mL) a 95% confidence interval of ± 6 mg/mL is reported in the D873 method.

The addition of antioxidants to DMF at the recommended concentration for gasoline (40 ppm total) provided a modest increase in the D525 breakpoint, raising it from 66 to 81 min, and had no significant impact on gum formation. Note that the 95% confidence interval for the breakpoint time is reported as ± 5% of the measured value in the D525 method. With an increase to 10 times the recommended antioxidant concentration (400 ppm), the DMF blend passed the D525 minimum breakpoint of 240 min; however, the amount of gum formed over 24 h was not significantly changed. The recommended antioxidant concentration for gasoline is intended to stabilize the fuel against oxidation of heavy di-olefins that would be present at 0.5–1 vol% [27], while the blends tested here contain an order of magnitude higher concentration of compounds susceptible to oxidation.

DMF and MF were allowed to evaporate in a fume hood at ambient conditions. In the case of MF, this took approximately 4 days and DMF took approximately 7 days given its higher boiling point. After evaporation, gums were visible in the bottoms of the flasks (Fig. 2). Given

Table 3
Qualitative GC–MS results as percent of total area from analysis of dissolved gums and decanted liquid following 24 h at 100 °C under 700 kPa initial O_2 pressure (ND = not detected).

Tentative ID	Molecular weight	Structure	DMF gum	DMF isooctane	MF gum	MF isooctane	EF gum	EF isooctane
2(3H)-Furanone, 5-methyl-	98	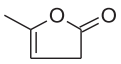	ND	ND	2.7	8.5	ND	ND
5-Methylfurfural	110	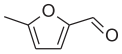	0.9	ND	2.0	ND	ND	ND
Ethanone, 1-(2-furanyl)-	110		ND	ND	ND	ND	2.6	1.4
4-Oxopentanoic acid	116	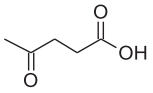	ND	ND	30.8	ND	ND	ND
Furan, 2,2′-methylenebis[5-methyl-	176	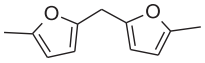	ND	1.6	0.7	6.9	ND	ND
4,4-bis(5-methylfuran-2-yl)butan-2-one	232	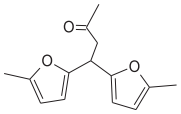	ND	ND	4.1	16.0	ND	ND
3-Hexene-2,5-dione (DAE)	112	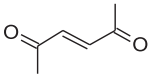	60.0	54.3	ND	ND	ND	ND
Methyl 4-oxo-2-pentenoate	128	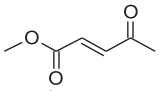	11.2	8.0	1.2	1.8	ND	ND
4-Oxohexanoic acid	130	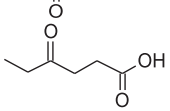	ND	ND	ND	ND	18.9	1.6
2-Butanone, 4-(5-methyl-2-furanyl)-	152	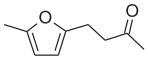	1.1	3.3	ND	ND	ND	ND
2-ethyl-5-[1-(furan-2-yl)ethyl]furan	190	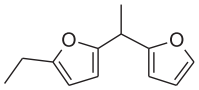	ND	ND	ND	ND	19.1	47.4
2,2′-ethane-1,1-diylbis(5-ethylfuran)	218	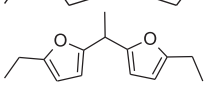	ND	ND	ND	ND	6.3	11.5

Table 4
GPC results of furanic oxidation gums.

Sample	Mp	Mn	Mw
MF gum	318	567	1087
DMF gum	233	581	1918
EF gum	294	561	2839

Mp = peak molecular weight, Mn = number average molecular weight, Mw = weight average molecular weight.

the possibility of reactive organic peroxide formation [25], these samples were handled with caution to prevent shock until taken up in a solvent for analysis.

3.2. Oxidation product characterization

Iso-octane insoluble gums formed by MF, DMF, and EF after 24 h of exposure to 100 °C and 700 kPa initial O_2 pressure were found to be readily soluble in THF and acetone. The small amount of gum formed by furan was not soluble in any typical solvent attempted (acetone, THF, dimethylsulfoxide, acetonitrile, methanol, and diethyl ether). Due to a lack of solubility and the very small amount produced, the furan gum was not analyzed.

Gums dissolved in acetone as well as iso-octane/furanic compound blends recovered after 24 h of oxidation were analyzed by GC–MS to identify volatile and semi-volatile degradation components. The most abundant peaks detected along with their percent contribution to the total chromatographic area are shown in Table 3. The percent areas shown exclude solvents and the parent furan compounds to qualitatively compare the relative abundances of products only. Matches to the National Institute of Standards and Technology database with a minimum of 75% confidence were considered for identifications and visual inspection of each mass spectrum was conducted to confirm the likelihood of correctly assigned structure. These assignments are tentative as standards were not injected to confirm retention times and spectra. A complete listing of peaks for each chromatogram with match qualities is provided in Tables S-1 to S-6, and in Figs. S-1 and S-2 showing mass spectra of manually assigned compounds, in the supporting information.

For DMF, the predominant volatile/semivolatile component, contributing over 50% of the chromatographic area for both the liquid and gum, was identified as 3-hexene-2,5-dione (1,2-diacetylethylene, DAE) by mass spectra matching. Analysis of the gum by ^{13}C NMR confirmed this compound identification as a primary component. The ^{13}C NMR spectrum is provided in Fig. S-3 in the supporting information along with more detailed results of spectrum integration and analysis. Levulinic acid methyl ester (methyl 4-oxo-2-pentenoate) was also observed at significant levels. 5-Methylfurfural was observed in the gum residue, and a DMF dimer was observed in the liquid phase.

Chromatograms of both EF and MF gums contained relatively large peaks identified as organic acids; 4-oxopentanoic acid in the case of MF (levulinic acid) and oxohexanoic acid in the case of EF. Neither of these organic acids appeared in high abundance in the iso-octane blends, likely due to the low solubility of the organic acids in the hydrocarbon matrix. For MF, low levels of 5-methylfurfural and 2-butanone, 4-(5-methyl-2-furanyl) indicate that reactive species can add at the 5-position of MF. Similarly for EF, 5-ethylfurfural is observed. Furanyl ethanone shows reaction of the side chain in EF. Compounds that preserve the furan ring and potentially form as furanic compound dimers and trimers, or reaction of a ring opening product with the parent furanic compound were also found in relatively high abundance in both the gums and liquid phase, especially for EF.

Gums dissolved in THF were analyzed by GPC to determine their molecular weight ranges. Results of this analysis are provided in Table 4. The molecular weights of these materials show a considerable increase in mass from the starting materials indicating further polymerization beyond the dimers detected by GC–MS. DART-TOF MS analysis was conducted to gain greater insight into the composition of the higher molecular weight fraction of the gums. These results are shown in Table S-7 in the Supporting information and suggest that higher molecular weight compounds present in the gums are likely composed of amorphous furanic polymers.

Neat MF and DMF were allowed to evaporate under ambient conditions in a fume hood, generating the gums shown in Fig. 2. These were dissolved in acetone and also analyzed by GC–MS. The results are provided in Table 5. DMF was again found to produce primarily DAE; however, there was also significant contribution from 5-methylfurfural and 5-methylfurfuryl alcohol. The highest concentration products for MF again suggest that a ring opening product reacted with the parent furan, but in this case 4-oxopentanoic acid was not detected. Peroxide titration was conducted on the gums produced by both MF and DMF to examine the possibility for shock sensitive peroxides. The gums produced by MF were found to contain a high concentration of peroxides, 2700 ± 500 ppm, while DMF gums contained 135 ± 20 ppm. Precision of the DMF gums analysis was determined from replicates of fuel samples within the range of 0–250 ppm peroxide. The precision stated for the MF gums is based on the difference between duplicate analyses. The nature of these peroxides is unknown thus the gums from these experiments were handled as potentially shock sensitive.

3.3. Oxidation mechanism

Sendt and coworkers and Vasiliou and coworkers studied the thermal decomposition of furan theoretically with correlated multi-reference CASPT2 and composite G2 (MP2) methods. Their work mainly focused on unimolecular decomposition pathways [32] and generation of propargyl radicals [33]. Several researchers have studied the gas phase oxidation mechanisms of DMF and MF under different flame

Table 5
Qualitative GC–MS results as percent of total area from analysis of gums from oxidation at ambient conditions (ND = not detected).

Tentative ID	Molecular weight	Structure	MF gum	DMF gum
Furfural	96	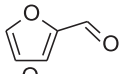	0.9	ND
2-Furanmethanol	98	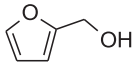	1.9	ND
2(3H)-Furanone, 5-methyl-	98	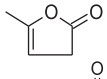	7.6	ND
1-(5-methylfuran-2-yl)pentane-1,4-dione	180	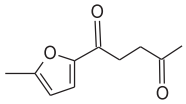	24.0	ND
(1E)-3,3-bis(5-methylfuran-2-yl)prop-1-en-1-ol	218	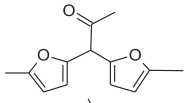	13.6	ND
(3E)-5,5-bis(5-methylfuran-2-yl)pent-3-en-2-one	244	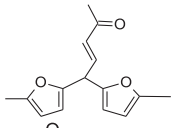	3.2	ND
5-Methylfurfural	110	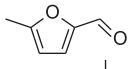	ND	4.1
3-Hexene-2,5-dione (DAE)	112	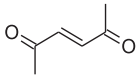	ND	55.6
5-Methylfurfuryl alcohol	112	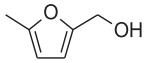	ND	3.6

conditions, temperatures, and pressures [34]. However, our experimental product distribution for the much lower temperature liquid-phase oxidation is quite different and cannot be directly compared to previously calculated mechanisms. Therefore, we propose mechanisms for DMF and MF liquid-phase oxidation to account for our different product distributions. The key experimental observations informing mechanism development were:

- No reaction occurs under nitrogen.
- Antioxidant additives at sufficient concentration inhibit the reaction.
- The furan blend did not react to form oxidation products.
- DMF reacts to form ring opening products (DAE, methyl 4-oxo-2-pentenoate, 5-methyl furfural, and furfural alcohol at room temperature) as well as dimerization products.
- MF and EF react to form both ring opening and condensation products that preserve the furan ring (4-oxo-pentanoic acid; 5-methyl-2(3H)-furanone; 4,4-bis(5-methylfuran-2-yl)butan-2-one; and similar compounds for MF; and 4-oxohexanoic acid, 2-ethyl-5-[1-(furan-2-yl)ethyl]furan and similar compounds for EF).
- The reaction products observed by GC–MS react further to produce higher molecular weight oligomers.

The bond dissociation energy of the furan ring's C—H bonds is among the strongest known (~120 kcal/mol); in contrast, the methyl C—H bond dissociation energy of DMF was calculated at 85 kcal/mol [11]. This value is lower than that of an allylic C—H bond of a polyunsaturated fatty acid (approximately 89 kcal/mol) [35], which is well known to undergo autoxidation via a free radical mechanism [36]. The 5-methyl-2-furanylmethyl radical species is an important primary radical in DMF combustion [37,38]. Thus, we initially examined reactions that involved breaking of the C—H bond in the alkyl group (Fig. 3).

The initial C—H cleavage from the methyl group in DMF could occur thermally to form **INT1_3**, by reaction with O_2, or by reaction with hydroxyl or hydroperoxy radicals formed by other reactions (shown in Fig. 3(a)), which is thermodynamically unfavorable by 32.8 kcal/mol. This radical species (**INT1_3**) can react with water, which is present at low levels in commercial fuels or formed as an oxidation reaction product, yielding **INT1_1**, which, as shown in Fig. 3, can initiate a ring opening cycle leading to DAE through **INT1_4** and **INT2_1** intermediates. The overall reaction has a favorable energy change of -87.4 kcal/mol, but the initial C—H abstractions step is highly endothermic. Alternatively, the initial radical **INT1_3** can react with oxygen to form an alkyl peroxide intermediate (**INT1_4**) that likely rapidly forms 5-methylfurfural (5MF) and ·OH. Low levels of 5-methylfurfural (from DMF), furfural (from MF), and 2-furanylethanone (from EF) suggest that reactions of the alkyl group to produce carbonyl species and OH radical are occurring in alkyl furan oxidation. These reactions may be the source of OH radicals that can lead to ring opening products, as described below. We believe furan does not undergo the ring opening reaction because there are no alkyl groups from which O_2 can abstract H to form the initial reactive OOH species which begins the radical chain mechanism. However, because these calculations show that C—H abstraction from an alkyl group is thermodynamically unfavorable, and so we considered other pathways.

In addition to forming by reaction of 5-methyl-2-furanylmethyl radical with water, **INT1_1** can, under lower temperature liquid-phase oxidation conditions, form directly by hydroxyl radical (·OH) addition to the π system at C2 (or C5). Fig. 4 shows a proposed mechanism for the overall reaction cycle of DMF and G4 potential energy profile. Hydroxyl radical addition is exothermic by 37.8 kcal/mol (shown in Fig. 4(b)), in part because the unpaired electron is delocalized over the furan ring. Addition at C3 or C4 has been shown to be much less energetically favorable [38]. Ferraz-Santos et al. reported that ·OH addition to DMF is important at lower temperatures, while H-abstraction becomes a competing pathway at typical combustion temperatures [39]. Additionally, ·OH addition to furan was proposed to explain products observed in studies of the reaction of furanic compounds in the atmosphere [40].

Homolytic C—O bond cleavage after OH radical addition gives the ring-opening product, **INT2_1**, via **TS1_1** with a 19.0 kcal/mol barrier height. Subsequently, H atom-abstraction from **INT2_1** by triplet dioxygen ($^3O_2$) in **TS2_1** (9.2 kcal/mol barrier) releases the (experimentally observed) DAE product, **DAE**. Our calculations show the unpaired electron in **INT2_1** is highly delocalized (see spin density plots in Fig. S-4 of the Supporting information), in agreement with the findings of Somers and coworkers [38]. This delocalization means that **INT2_1** is less susceptible towards radical recombination than e.g., a localized alkyl radical, favoring H atom-abstraction instead. The hydroperoxy radical (·OOH) generated can attack C2 (or C5) of a second **DMF** molecule, forming **INT1_2**, which is thermodynamically favorable by 47.4 kcal/mol. Similar to the first reaction, C—O bond cleavage proceeds through **TS1_2** to form **INT2_2**. The computed activation energy barrier in **TS1_2** is 20.7 kcal/mol, within 1.7 kcal/mol of the value calculated for reaction with OH radical (**TS1_1**). In the final step, **INT2_2** forms a second **DAE** product and regenerates the OH radical propagating the radical chain. This mechanistic profile is consistent with experimental findings, and the overall computed ΔE value is −56.8 kcal/mol.

Based on our mechanism from Fig.4, the overall reactions are given by Eq. (1) with two reactant molecules and O_2, composed of reactions (2) and (3). The hydroxyl radical acts as a chain-carrier.

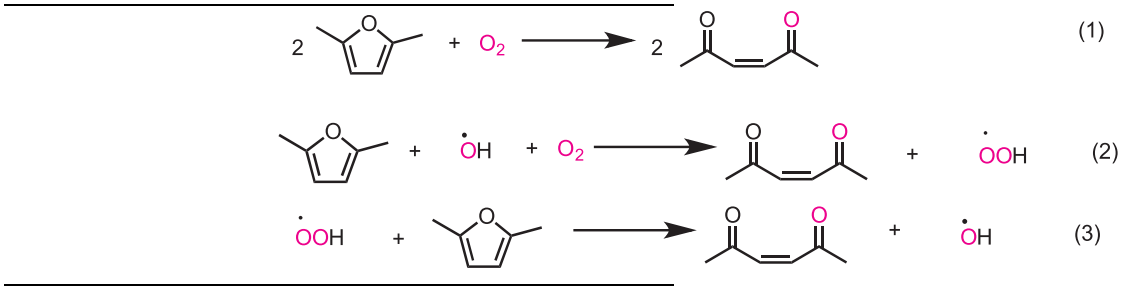

As noted, oxidation of alkyl groups on the furan ring by dioxygen is a viable source of low concentrations of OH radical for subsequent reactions. For MF this can lead to ring-opened products as shown in Fig. 5. Density functional theory calculations show that the overall reaction is similar to the DMF reactions producing **3AA** (4-keto-2-pentenal or 3-acetylacrolein). In addition to these ring-opened products, the GC–MS product distribution of MF in Table 3 also shows products from further condensation reactions. Comparable reactivity is not observed for the carbonyl products of DMF, readily attributable to the greater electrophilicity of the aldehyde moiety in **3AA** compared to the

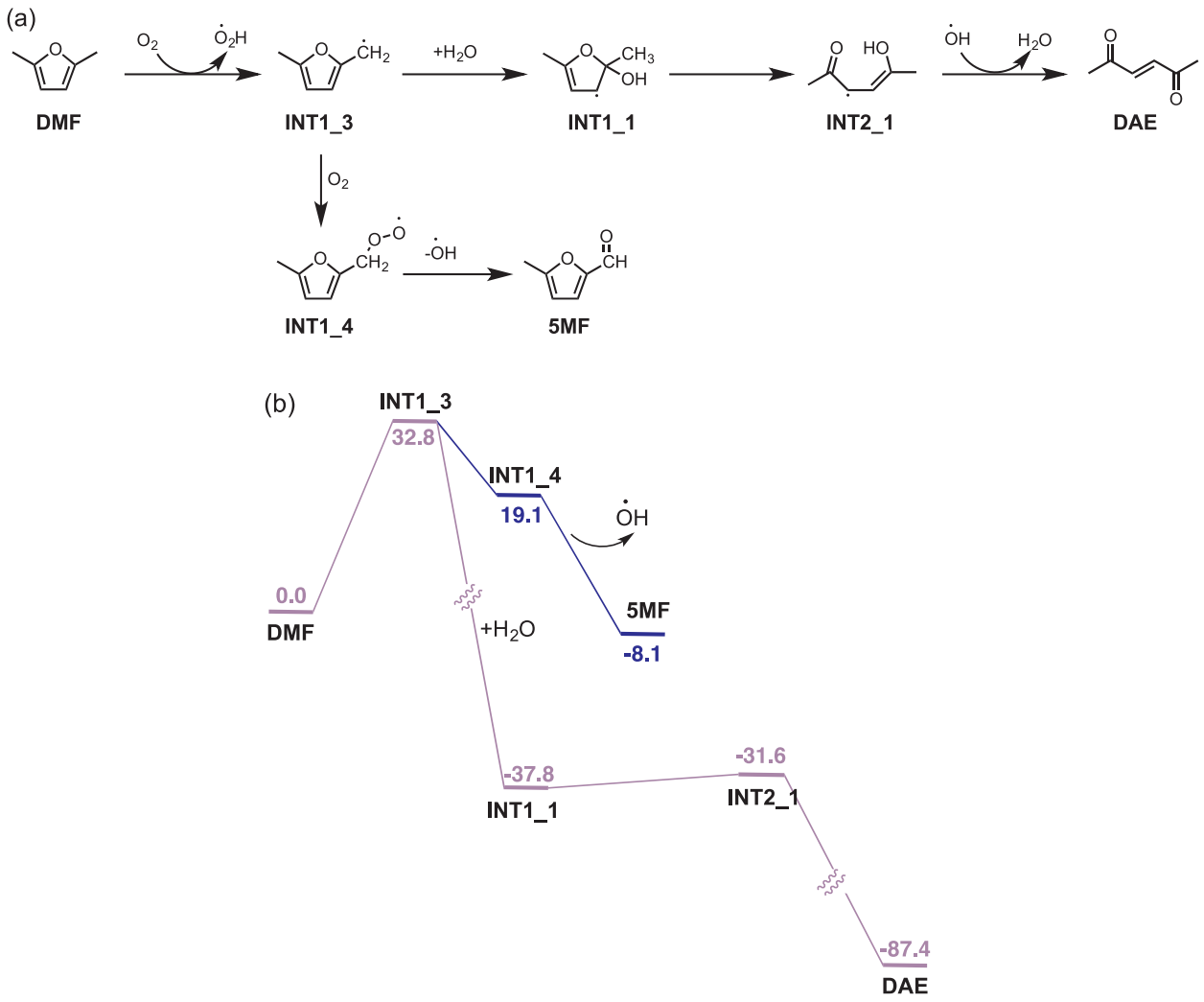

Fig. 3. (a) Proposed mechanisms and (b) potential energy surface for DMF reactions initiated through alkyl group C−H bond cleavage using G4 energies in kcal/mol.

less reactive ketone in **DAE**. The condensation of **3AA** with two additional MF molecules was computed (Fig. 6). The overall reaction is very favorable ($\Delta E = -20.5$ kcal/mol). All of the proposed elementary steps are energetically feasible. These reactions are similar to those described by Corma and coworkers for the coupling of 2 MF molecules with an aldehyde prior to hydrogenation to produce a hydrocarbon in the diesel boiling range [41]. Finally, we proposed that **3AA** can react with water and undergo isomerization via a 1,2-hydride shift to form 4-oxo-pentanoic acid (levulinic acid), which is observed as a significant reaction product (Table 3), as shown in Fig. 7.

4. Discussion

The results presented highlight the relatively high reactivity of alkyl furans compared to conventional gasoline at low temperatures with formation of polar reactive species, gums, and peroxides. Although the potential for shock sensitive peroxides has not been established it is likely that MF and DMF fall under Class B peroxide forming chemicals, meaning they may have the potential for hazardous peroxides to concentrate upon evaporation or distillation [26]. Many common laboratory solvents fall within this classification, including diethyl ether and isopropyl alcohol, thus safe handling practices are typically established in research facilities including periodic monitoring for peroxides and limitations on storage time. These precautions are advised when conducting research on these oxygenates.

Given the otherwise highly desirable fuel properties of DMF and MF for use as gasoline blend components, it is important to understand whether these negative stability results are a problem that can be overcome, or if they make these potential new fuels practically and economically untenable. The stability tests were conducted at 100 °C under 700 kPa initial oxygen pressure, which are the conditions of the ASTM D525 gasoline oxidation stability test. Like many fuel specification tests, the ASTM D525 test was developed based on an approximate correlation developed using data on conventional gasolines. As stated in the test method: “The induction period may be used as an indication of the tendency of motor gasoline to form gum in storage. It should be recognized, however, that its correlation with the formation of gum in storage may vary markedly under different storage conditions and with different gasolines [42].” Blends containing 10 vol% or more of a furanic compound are clearly not similar to the conventional gasolines used in creating the D525 test method and should be considered even more subject to these caveats. However, given the very short induction time observed for the DMF blend and the very high levels of gum formation observed for both DMF and MF, it seems unlikely that the approximate nature of the D525 test correlation opens a window to allow a claim that the furanic blend components are in fact adequately stable. The observation that the 10% MF blend met the gasoline induction time requirement of 240 min minimum, but at the same time formed roughly two orders of magnitude more gum than might be found in a conventional gasoline suggests that if the D525 test is inappropriate for MF, it is because it fails to predict gum formation based on induction time. All of this discussion strongly argues that the poor oxidation stability of the

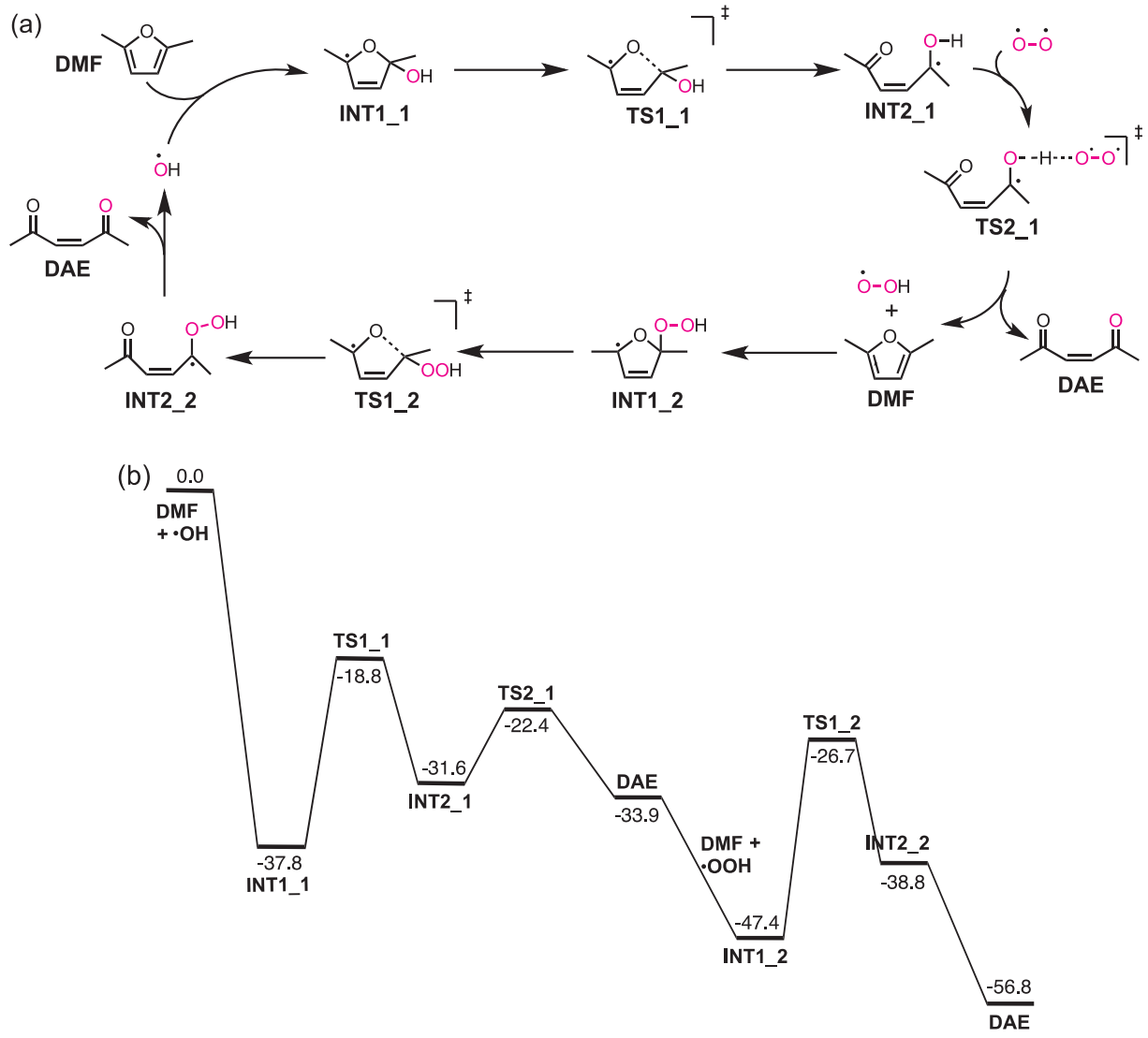

Fig. 4. (a) Proposed mechanism and (b) potential energy diagram for DAE formation from DMF via oxidation. G4 energies in kcal/mol relative to DMF.

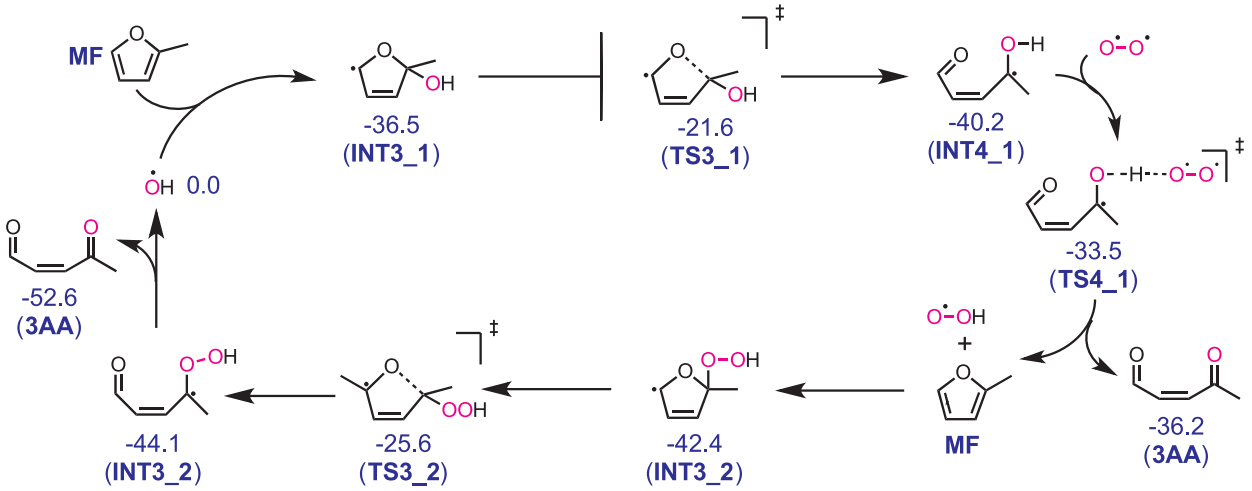

Fig. 5. Proposed mechanism for 3-acetylacrolein formation from MF via oxidation. Computed energies are shown for each species. B3LYP/6-31G(2df,p) energies shown in kcal/mol relative to MF.

DMF and MF blends may make these blend components unworkable from a practical standpoint.

Conventional gasolines, including ethanol blends, are routinely treated with antioxidant additives to prevent gum formation that largely originates from olefinic and diolefinic components [27]. In this study, a commercial gasoline antioxidant had only a small effect on the

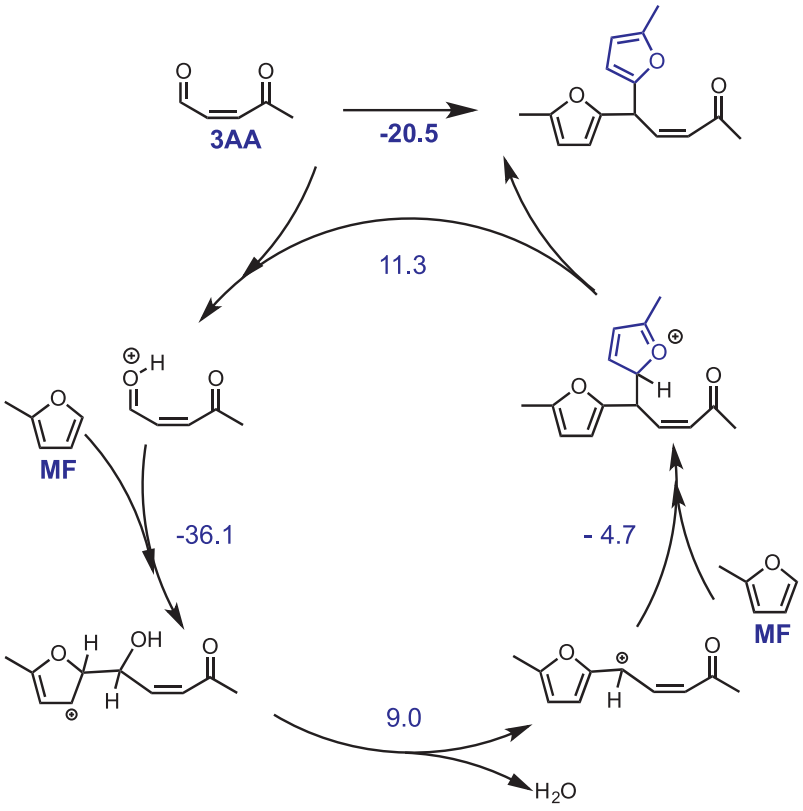

Fig. 6. Proposed condensation mechanism of MF and 3AA (3-acetylacrolein). B3LYP/6-31G(2df,p) energies shown in kcal/mol relative to MF and 3AA.

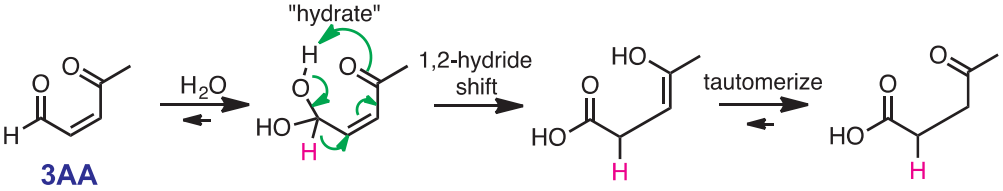

Fig. 7. Formation of 4-oxo pentanoic acid from 4-keto-2-pentenal.

DMF blend induction time at the standard treat rate of 40 ppm, but did significantly improve induction time at 400 ppm. Nevertheless, antioxidant treatment had little impact on gum formation. One reason for the poor effectiveness of the antioxidant additive is that in conventional gasoline the diolefins may only be present at a few volume percent while here the reactive furanic component is present at 10 vol%. Another reason could be that the conventional gasoline antioxidants are not tuned for the reactive furanic species. The primary mode of action of hindered phenolic antioxidants is to donate a proton to an organic peroxide species, interrupting the chain reaction cycle and forming a very stable radical [43]. The phenolic O—H bond dissociation energy and other properties can be tuned to create antioxidants that are tailored for the substance being treated. Furthermore, proton capping of a peroxide species such as **INT1_4** in Fig. 3 may not prevent that species from reacting further. Finally, the catalytic cycles described in Figs. 4 and 6 exhibit species that are significantly different from those observed in more conventional autoxidation reactions and the reactions may not be amenable to interruption by traditional gasoline antioxidants. Thus, it remains a possibility that an appropriate antioxidant additive or a combination of additives can halt the low temperature oxidation of furanic compounds, and developing or identifying such an antioxidant should be the focus of future research in this area.

5. Conclusions

Alkylated furanics have promising spark-ignition fuel properties that make them attractive renewable fuel blendstocks. The results of this study show that these compounds have low oxidative stability forming highly polar compounds that can react further to form polymers. Gum levels for 10 vol% blends were 10–100 times higher than seen for on specification conventional gasolines. Peroxides were observed to be present in gums formed under ambient conditions. It is undetermined whether these pose a shock hazard; therefore caution is recommended when conducting experiments in which these compounds are to be evaporated or distilled. The use of common antioxidants was shown to improve the oxidative stability of DMF; however, this required a fairly large concentration of additives that did not prevent the formation of gum after 24 h of oxidation. The relatively poor stability of these compounds will likely limit the concentration that can be blended into gasoline as well as necessitate relatively high concentrations of antioxidants to prevent degradation, unless improved antioxidants tailored specifically to the important oxidation intermediates can be developed.

Acknowledgements

This research was conducted as part of the Co-Optimization of Fuels & Engines (Co-Optima) project sponsored by the U.S. Department of Energy – Office of Energy Efficiency and Renewable Energy, Bioenergy Technologies and Vehicle Technologies Offices. Co-Optima is a collaborative project of several national laboratories initiated to simultaneously accelerate the introduction of affordable, scalable, and sustainable biofuels and high-efficiency, low-emission vehicle engines. Work at the National Renewable Energy Laboratory was performed

under Contract No. DE347AC36-99GO10337. Computer time was provided by the Texas Advanced Computing Center under the National Science Foundation Extreme Science and Engineering Discovery Environment Grant MCB-090159 and by the National Renewable Energy Laboratory Computational Sciences Center. The U.S. Government retains and the publisher, by accepting the article for publication, acknowledges that the U.S. Government retains a non-exclusive, paid-up, irrevocable, worldwide license to publish or reproduce the published form of this work, or allow others to do so, for U.S. Government purposes.

Appendix A. Supplementary data

Supplementary data associated with this article can be found, in the online version, at http://dx.doi.org/10.1016/j.fuel.2017.10.066.

References

[1] Christensen E, Yanowitz J, Ratcliff M, McCormick RL. Renewable oxygenate blending effects on gasoline properties. Energy Fuels 2011;25:4723–33.
[2] McCormick RL, Fioroni GM, Fouts L, Christensen E, Yanowitz J, Polikarpov E, Albrecht K, Gaspar DJ, Gladden J, George A. Selection criteria and screening of potential biomass-derived streams as fuel blendstocks for advanced spark-ignition engines. 2017;10(2). http://dx.doi.org/10.4271/2017-01-0868.
[3] Bohre A, Dutta S, Saha B, Abu-Omar MM. Upgrading furfurals to drop-in biofuels: an overview. ACS Sustainable Chem. Eng 2015;3:1263–77.
[4] Lessard J, Morin JF, Wehrun JF, Magnin D, Chornet E. High yield conversion of residual pentoses into furfural via zeolite catalysis and catalytic hydrogenation of furfural to 2-methylfuran. Top Catal 2010;53:1231–4.
[5] Roman-Leshkov Y, Barrett CJ, Liu ZY, Dumesic JA. Production of dimethylfuran for liquid fuels from biomass-derived carbohydrates. Nature 2007;447:982–5.
[6] Schmidt LD, Dauenhauer PJ. Chemical engineering: hybrid routes to biofuels. Nature 2007;447:914–5.
[7] Binder JB, Raines RT. Simple chemical transformation of lignocellulosic biomass into furans for fuels and chemicals. J Am Chem Soc 2009;131:1979–85.
[8] Nilges P, Schroder U. Electrochemistry for biofuel generation: production of furans by electrocatalytic hydrogenation of furfurals. Energy Environ Sci 2013;6:2925–31.
[9] Zhang J, Lin L, Liu S. Efficient production of furan derivatives from a sugar mixture by catalytic process. Energy Fuels 2012;26:4560–7.
[10] Wang J, Liu X, Hu B, Lu G, Wang Y. Efficient catalytic conversion of lignocellulosic biomass into renewable liquid biofuels via furan derivatives. RSC Adv 2014;4:31101–7.
[11] Simmie JH, Curran HJ. Formation enthalpies and bond dissociation energies of alkylfurans. the strongest C- X bonds known? J Phys Chem A 2009;113:5128–37.
[12] Simmie JH, Metcalf WK. Ab initio study of the decomposition of 2,5-dimethylfuran. J Phys Chem A 2011;115:8877–88.
[13] Sirjean B, Fournet R, Glaude P-A, Battin-Leclerc F, Wang W, Oehlschlaeger M. Shock Tube and chemical kinetic modeling study of the oxidation of 2,5-dimethylfuran. J Phys Chem A 2013;117:1371–92.
[14] Xu N, Tang C, Meng X, Fan X, Tian Z, Huang Z. Experimental and kinetic study on the ignition delay times of 2,5-dimethylfuran and the comparison to 2-methylfuran and furan. Energy Fuels 2015;29:5372–81.
[15] Alexandrino K, Millera A, Bilbao R, Alzueta MU. Novel aspects in the pyrolysis and oxidation of 2,5-dimethylfuran. Proc Combust Inst 2015;35:1717–25.
[16] Zhong S, Daniel R, Xu H, Zhang J, Turner D, Wyszynski ML, et al. Combustion and Emissions of 2,5-Dimethylfuran in a Direct-Injection Spark-Ignition Engine. Energy Fuels 2010;24:2891–9.
[17] Daniel R, Tian G, Xu H, Wyszynski ML, Wu X, Huang Z. Effect of spark timing and load on a DISI engine fuelled with 2,5-dimethylfuran. Fuel 2011;90:449–58.
[18] Thewes M, Muether M, Pischinger S, Budde M, Brunn A, Sehr A, et al. Analysis of the impact of 2-methylfuran on mixture formation and combustion in a direct-injection spark-ignition engine. Energy Fuels 2011;25:5549–61.
[19] Rothamer DA, Jennings JH. Study of the knocking propensity of 2,5-dimethylfuran–gasoline and ethanol–gasoline blends. Fuel 2012;98:203–12.
[20] Hoppe F, Burke U, Thewes M, Heufer A, Kremer F, Pischinger S. Tailor-made fuels from biomass: potentials of 2-butanone and 2-methylfuran in direct injection spark ignition engines. Fuel 2016;167:106–17.
[21] Ratcliff MA, Burton J, Sindler P, Christensen E, Chupka GM, Fouts L, McCormick RL. Knock resistance and fine particle emissions for several biomass-derived oxygenates in a direct-injection spark-ignition engine. 2016;9(1). http://dx.doi.org/10.4271/2016-01-0705.
[22] American Society for Testing Materials, “ASTM Special Publication No. 225: Knocking Characteristics of Pure Hydrocarbons”, May 1958, http://www.astm.org/DIGITAL_LIBRARY/STP/SOURCE_PAGES/STP225_foreword.pdf.
[23] Lange J-P, van der Heide E, van Buijtenen J, Price R. Furfural – a promising platform for lignocellulosic biofuels. ChemSusChem 2012;5:150–66.
[24] McCormick RL, Ratcliff M, Christensen E, Fouts L, Luecke J, Chupka GM, et al. Properties of oxygenates found in upgraded biomass pyrolysis oil as components of spark and compression ignition engine fuels. Energy Fuels 2015;29:2453–61.
[25] Fabos V, Koczo G, Mehdi H, Boda L, Horvath T. Bio-oxygenates and the peroxide number: a safety issue alert. Energy Environ Sci 2009;2:767–9.
[26] National Research Council. Prudent Practices for Handling Hazardous Chemicals in Laboratories. Washington, D.C.: National Academy Press; 2005.
[27] Pradelle F, Braga SL, Martins ARFA, Turkovics F, Padelle RNC. Gum formation in gasoline and its blends: a review. Energy Fuels 2015;29:7753–70.
[28] Curtiss LA, Redfern PC, Raghavachari K. Gaussian-4 theory. J Chem Phys 2007;126:084108.
[29] Rayne S, Forest K. Estimated gas-phase standard state enthalpies of formation for organic compounds using the gaussian-4 (g4) and w1bd theoretical methods. J Chem Eng Data 2010;55:5359–64.
[30] Simmie JM. A database of formation enthalpies of nitrogen species by compound methods (CSB-QB3, CBS-APNO, G3, G4). J Phys Chem A 2015;119:10511–26.
[31] Frisch MJ, Trucks GW, Schlegel HB, Scuseria GE, Robb MA, Cheeseman JR, et al. Gaussian 09. Wallingford, CT: Gaussian Inc; 2009.
[32] Sendt K, Bacskay GB, Mackie JC. Pyrolysis of furan: ab initio quantum chemical and kinetic modeling studies. J Phys Chem A 2000;104:1861–75.
[33] Vasiliou A, Nimlos MR, Daily JW, Ellison GB. Thermal decomposition of furan generates propargyl radicals. J Phys Chem A 2009;113:8540–7.
[34] Badovskaya LA, Pavarova LV. Oxidation of furans (review). Chem Heterocycl Compd 2009;45:1023–34.
[35] Blanksby SJ, Ellison GB. Bond dissociation energies of organic molecules. Acc Chem Res 2003;36:255–63.
[36] Frankel EN. Lipid Oxidation. Dundee, Scotland: The Oily Press; 1998.
[37] Sirjean B, Fournet R. Theoretical study of the thermal decomposition of the 5-methyl-2-furanylmethyl radical. J Phys Chem A 2012;116:6675–84.
[38] Somers KP, Simmie JM, Gillespie F, Conroy C, Black G, Metcalf WK, et al. A comprehensive experimental and detailed chemical kinetic modelling study of 2,5-dimethylfuran pyrolysis and oxidation. Comb Flame 2013;160:2291–318.
[39] T. Ferraz-Santos, G.F. Bauerfeldt, Ab Initio Study of the Reactions of OH radical with 2,5,-Dimethylfuran. Proceedings of the European Combustion Meeting, 2015.
[40] Aschmann SM, Nishino N, Arey J, Atkinson R. Kinetics of the reactions of OH radicals with 2- and 3-Methylfuran, 2,3- and 2,5-Dimethylfuran, and E- and Z-3-Hexene-2,5-dione, and products of OH þ 2,5-dimethylfuran. Environ Sci Tech 2011;45:1859–65.
[41] Corma A, de la Torre O, Renz M. Production of high quality diesel from cellulose and hemicellulose by the sylvan process: catalysts and process variables. Energy Environ Sci 2012;5:6328–44.
[42] ASTM D525-12a. Standard Test Method for Oxidation Stability of Gasoline (Induction Period Method). West Conshohocken, PA: ASTM International; 2012. www.astm.org.
[43] Yehye WA, Rahman NA, Ariffin A, Hamid SBA, Alhadi AA, Kadir FA, et al. Understanding the chemistry behind the antioxidant activities of butylated hydroxytoluene (bht): a review. Eur J Med Chem 2015;101:295–312.